International Conference on Space Optics—ICSO 2014

La Caleta, Tenerife, Canary Islands

7–10 October 2014

Edited by Zoran Sodnik, Bruno Cugny, and Nikos Karafolas

METIS: the visible and UV coronagraph for solar orbiter

M. Romoli

F. Landini

E. Antonucci

V. Andretta

et al.

International Conference on Space Optics — ICSO 2014, edited by Zoran Sodnik, Nikos Karafolas, Bruno Cugny, Proc. of SPIE Vol. 10563, 105631M · © 2014 ESA and CNES
CCC code: 0277-786X/17/$18 · doi: 10.1117/12.2304274

METIS: THE VISIBLE AND UV CORONAGRAPH FOR SOLAR ORBITER

M. Romoli[1], F. Landini[2], E. Antonucci[3], V. Andretta[4], A. Berlicki[5], S. Fineschi[3], J. D Moses[6], G. Naletto[7], P. Nicolosi[7], G. Nicolini[3], D. Spadaro[8], L. Teriaca[9], C. Baccani[1], M. Focardi[2], M. Pancrazzi[2], S. Pucci[1], L. Abbo[3], A. Bemporad[3], G. Capobianco[3], G. Massone[3], D. Telloni[3], E. Magli[10], V. Da Deppo[11], F. Frassetto[11], M.G. Pelizzo[11], L. Poletto[11], M. Uslenghi[12], S. Vives[13], M. Malvezzi[14]

[1] Department of Physics and Astronomy – University of Florence, Florence, Italy
MR: romoli@arcetri.astro.it; CB: cristianbaccani@libero.it; SP: stpucci@arcetri.astro.it
[2] INAF – Osservatorio Astrofisico di Arcetri – Florence, Italy
FL: flandini@arcetri.astro.it; MF: mauro@arcetri.astro.it; MP: panc@arcetri.astro.it
[3] INAF – Osservatorio Astrofisico di Torino, Pino Torinese, Italy
EA: antonucci@oato.inaf.it; SF: fineschi@oato.inaf.it; GN: nicolini@oato.inaf.it; LA: abbo@oato.inaf.it; AB: bemporad@oato.inaf.it; GC: capobianco@oato.inaf.it; GM: massone@oato.inaf.it; DT: telloni@oato.inaf.it
[4] INAF – Osservatorio Astronomico di Capodimonte, Napoli, Italy, VA: andretta@oacn.inaf.it
[5] Astronomical Institute of the Academy of Sciences, Ondrejov, Czech Republic, AB: arkadiusz.berlicki@asu.cas.cz
[6] Naval Research Laboratory, Washington D.C., USA, JM: moses@nrl.navy.mil
[7] Department of Information Engineering, University of Padova, Padova, Italy
GN: naletto@dei.unipd.it; PN: nicolosi@dei.unipd.it
[8] INAF - Osservatorio Astrofisico di Catania, Catania, Italy, DS: spadaro@oact.inaf.it
[9] Max-Plank- Institute für Sonnensystemforschung, Goettingen, Germany, LT: teriaca@mps.mpg.de
[10] Politecnico di Torino, Torino, Italy, EM: enrico.magli@polito.it
[11] CNR-Institute for Photonics and Nanotechnologies, Padova, Italy
VD: dadeppo@dei.unipd.it; FF: frassetto@dei.unipd.it; MP: pelizzo@dei.unipd.it; GP: poletto@dei.unipd.it
[12] INAF-IASF, Milano, Italy, MU: uslenghi@iasf-milano.inaf.it
[13] Aix Marseille Université, CNRS, LAM, Marseille, France; sebastien.vives@lam.fr
[14] University of Pavia, Pavia, Italy, MM: andreamarcomalvezzi@gmail.com

Abstract **-- METIS coronagraph is designed to observe the solar corona with an annular field of view from 1.5 to 2.9 degrees in the visible broadband (580-640 nm) and in the UV HI Lyman-alpha, during the Sun close approaching and high latitude tilting orbit of Solar Orbiter. The big challenge for a coronagraph is the stray light rejection. In this paper after a description of the present METIS optical design, the stray light rejection design is presented in detail together with METIS off-pointing strategies throughout the mission. Data shown in this paper derive from the optimization of the optical design performed with Zemax ray tracing and from laboratory breadboards of the occultation system and of the polarimeter.**

I. INTRODUCTION

The Multi-Element Telescope for Imaging and Spectroscopy - METIS – for the Solar Orbiter mission is designed to perform coronagraphic multi-wavelength imaging of the solar corona in the visible and, for the first time, in the UV. METIS can simultaneously image the visible and ultraviolet emission of the solar corona and diagnose, with unprecedented temporal coverage and spatial resolution the structures and dynamics of the full corona in the field-of-view (FOV) range from 1.5º to 2.9º. This corresponds to a range from 1.6 to 3.0 solar radii ($R_\odot$), at minimum perihelion (0.28 AU), and from 2.8 to 5.5 $R_\odot$, at 0.5 AU. METIS will be capable of obtaining:

- simultaneous imaging of the full corona in
  - linearly polarized visible-light (580-640 nm)
  - narrow-band ultraviolet HI Lyman α (121.6 nm)

with high temporal cadence (up to 1 s in visible-light; up to 5 min. in the UV), and plate scale (20 arcsec in the UV, and 10 arcsec in the visible).These measurements will allow a characterization of the main physical parameters (i.e., density, temperature and outflow velocities) and of the two most important plasma components of the corona and the solar wind (electrons, protons).
METIS instrument has been conceived to perform off-limb and near-Sun coronagraphy, with the aim of addressing the three key scientific issues concerning:

- the origin and heating/acceleration of the fast and slow solar wind streams;
- the origin, acceleration and transport of the solar energetic particles;

- and the transient ejection of coronal mass (coronal mass ejections - CMEs) and its evolution in the inner heliosphere.

The near-Sun multi-wavelength coronal imaging performed with METIS, combined with the unique opportunity offered by the Solar Orbiter mission profile, can effectively address and answer these issues, significantly improving our understanding of the region connecting the Sun to the heliosphere and the comprehension of the processes generating and driving the solar wind and CMEs.
Solar Orbiter will be launched in July 2017 (nominal date) and after a cruise phase of approximately 3 years it will start its 7.5 years-long nominal mission phase during which it will orbit the Sun in about 6 months and will achieve perihelion distances down to 0.28 Astronomical Units (AU).
Hereafter, a description of the present METIS design with its optical performance and stray light rejection after a re-scoping of the instrument in early 2013 [1].

II. INSTRUMENT DESCRIPTION

METIS is an externally occulted coronagraph. The advantage of an externally occulted coronagraph to observe the extended solar corona is given by the need of reducing the large dynamic range of the coronal signal that decreases exponentially from the limb to the outer corona. The highly vignetted aperture of the externally occulter coronagraph at lower heliocentric height compensates in part the high dynamic range, making possible the observation of the corona at higher heights. The occultation scheme is based on an inverted external-occulter (IEO).
The inverted external occulter (IEO) consists of a circular aperture (∅ 40 mm) (entrance pupil of the instrument) at the narrow end of a truncated cone (for stray light optimization) kept by a boom at 800 mm in front of the telescope. The disk-light through the IEO is rejected back by a spherical heat-rejection mirror (M0 - ∅ 71 mm) up to 1.1° (i.e., 1.17 $R_{\odot}$ at 0.28 AU). The coronal light, on the other hand, is collected by an on-axis Gregorian telescope. The suppression of the diffracted light off the edges of the IEO and M0 is achieved, respectively, with an internal occulter (IO) and a Lyot trap (LS).
The main motivation of adopting the original inverted-occultation scheme has been the need to reduce the thermal load in the instrument during perihelion operations. A classical externally-occulted coronagraph has an annular aperture defined by the entrance aperture and the outer edge of a disk that acts as external occulter. The telescope objective optics is in the shadow of the external occulter disk. For the same light-collecting area, a classical externally-occulted coronagraph requires an (annular) disk-light rejecting mirror that is much larger than the (circular) one used in the inverted-occultation scheme adopted for METIS. This reduces considerably (by two orders of magnitude) the thermal load on the rejection mirror.
The VL and UV paths are split by a UV interference filter at 12° angle of inclination with respect to the optical axis. The MgF_2+Al coatings in the primary (M1) and secondary (M2) telescope mirrors are optimized for enhanced reflectivity at 121.6 nm. The coating has also high reflectivity in the visible-light (580-640 nm). The UV narrow bandpass interference filter acts as VL-UV beam splitter by selecting the 121.6 nm UV band in transmission and reflecting the VL to the polarimeter. Inside the polarimeter a broad band filter selects the VL bandpass (580-640 nm). ***Fig. 1*** shows the ray-trace of the inverted-occultation coronagraph for the UV path.
The external occultation design advantages are that the telescope observes upto higher heliocentric heights, several solar radii, because the external occulter rejects the solar disk light in a more efficient way; in addition to that, the vignetting effect of the external occulter varies gradually the aperture of the telescope from zero, at the bottom end of the FOV, to a maximum value, at the top end of the FOV, as shown in ***Fig. 2***.

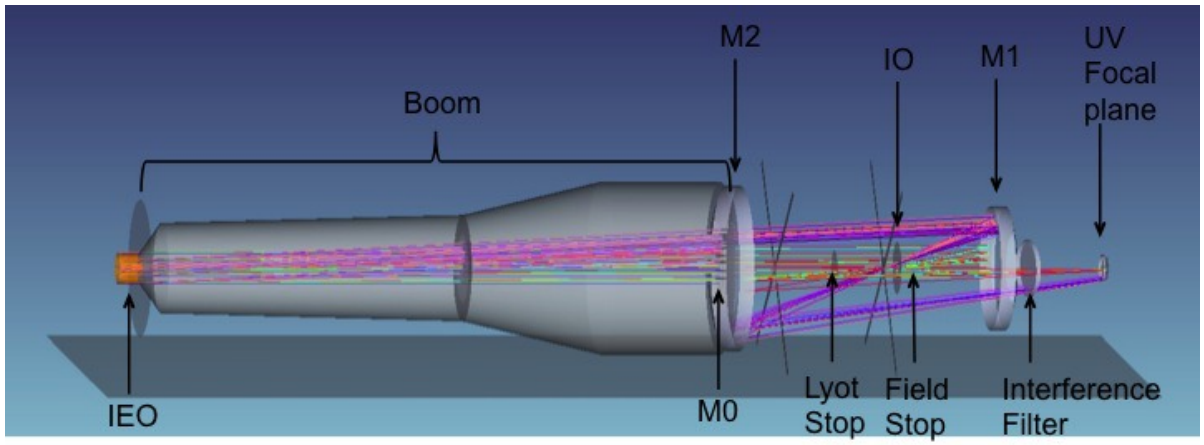

Fig. 1 - Schematic layout of METIS UV path.

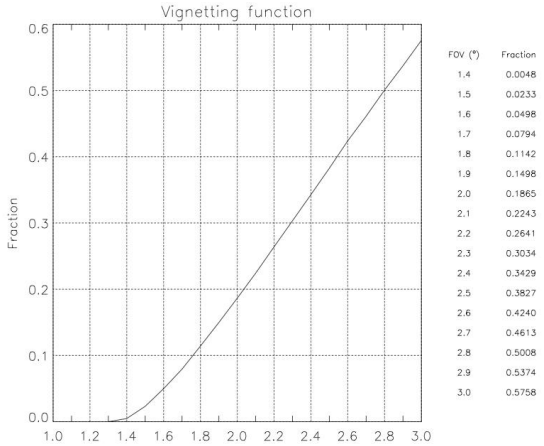

Fig. 2 - Vignetting function as a fraction of the entrance pupil defined by the IEO aperture as a function of the field angle.

The UV and VL detectors are, respectively, an intensified active pixel sensor (IAPS) with scale factor 20 arcsec/pixel and image size: 30.7 mm (1024x1024) with 30 µm equivalent pixel size; and an APS with scale factor 10 arcsec/pixel and image size: 20.5 mm (2048x2048) with 10 µm pixel size.
Table 1 summarizes the METIS top-level instrument performance aimed at satisfying the top-level observational requirement.

Table 1 - METIS instrument performance.

METIS Instrument Performance	
CORONAL IMAGING	
Wavelength range	VL: 580-640 nm; UV: 121.6 ± 10 nm
Effective focal length	VL: 200 mm; UV: 300 mm
Spatial Plate scale	10 arcsec (VL); 20 arcsec (UV)
Field of view	1.5° - 2.9° annular, off-limb corona ⇒1.6 - 3.0 $R_\odot$ @ 0.28 AU (min. perihelion) ⇒ 2.8 - 5.5 $R_\odot$ @ 0.5 AU
Average Instrumental Stray Light (stray-light to solar-disk irradiance ratio ≡ $B_{stray}/B_\odot$)	$B_{stray}/B_\odot$ (VL) $<10^{-9}$ $B_{stray}/B_\odot$ (UV) $<10^{-7}$

Temporal resolution	VL: 1-450 s UV: 1-30 min.
Broad-band Linear Polarization Sensitivity	≤ 10^{-2}
Signal-to-Noise Ratio	VL > 7 (7-590) UV > 3 (3-86)
GENERAL	
Telemetry rate	10.5 kbit/s
Data volume (compression up to 10)	27.2 Gb/orbit

A. VL polarimetry

METIS visible-light polarimeter [2] is designed to measure the linearly polarized solar K-corona in the Visible Light (VL) band 580 – 640 nm with a sensitivity to the fractional linear polarization measurement (i.e., minimum detectable linear polarization) better than or equal to 0.01.
The VL path polarimeter consists of a polarimetric group (PG) and a relay-optics system (ROS). The ROS collimates, through the PG, the light from the image formed by the telescope on the intermediate VL focal plane. Then the ROS re-focuses the image on the VL detector, with a 1:0.67 demagnification ratio to match the telescope plate scale with the APS pixel size. The PG electro-optically modulates the intensity of the linearly polarized K-corona. The PG is comprised of polarization optics in "Senarmont configuration":

i. bandpass (BP) filter (580-640 nm);
ii. fixed quarter-wave (QW) retarder;
iii. Polarization Modulation Package (PMP) with Liquid Crystal Variable Retarder (LCVR) double-cell;
iv. linear polarizer (LP).

Fig. 3 shows the optical layout of the VL path. The estimated instrumental polarization of the polarimeter is < $(5\pm1)\times10^{-2}$.
The theoretical demodulation matrix, necessary to compute the linear polarization Stokes image vector, S, from the 4 individual polarized images M ($S = X^{+} M$) is:

$$X^{+} = \frac{1}{2}\begin{pmatrix} 1 & 1 & 1 & 1 \\ 0 & -2 & 0 & 2 \\ -2 & 0 & 2 & 0 \end{pmatrix}$$

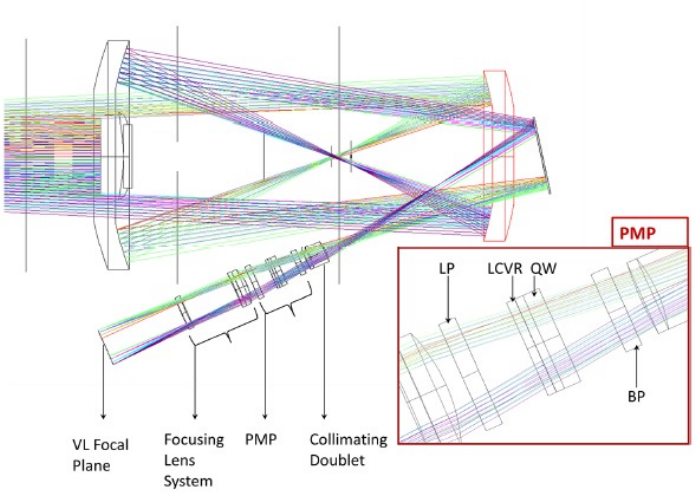

Fig. 3 - Optical layout for the visible light path.

III. METIS STRAY LIGHT REJECTION

METIS occultation scheme is based on an inverted external-occulter (IEO). The IEO consists of a truncated cone shaped aperture (see [3] for the detailed design) with an external circular aperture (∅ 40 mm). A spherical mirror (M0) (∅ 71 mm) rejects back the disk-light through the IEO up to 1.1° (i.e., 1.17 $R_\odot$ at 0.28 AU).
The goal of the METIS design is to achieve a level of in- and off-band stray-light suppression of:

- **VL:** B_{stray} (in- and off-band) < 10^{-9} $B_\odot$ (VL: 580 – 640 nm**)**
- **UV:** B_{stray} (in- and off-band) < 10^{-7} $B_\odot$ (UV: 115 – 130 nm)

where B_{stray} represents the stray light irradiance (photons cm^{-2} s^{-1}) measured on the telescope focal plane and $B_\odot$ represents the solar disk mean irradiance that would impinge on the focal plane as if the solar disk would extend throughout METIS FOV.
Note that "off-band" means outside the specified wavelength range. Both VL and UV wavelength bands can be affected by off-band stray-light. UV off-band stray light is mainly due to broadband visible light radiation. The narrowband Al+MgF_2 interference filter and the solar blind MCP of the UVD take care of the VL stray light. VL off-band stray light is mainly due to broadband visible light radiation outside the VL channel bandpass range. The passband filter takes care of the VL stray light.
The main source of stray-light in a coronagraph is the diffraction off the first element illuminated by the sun-disk light. For an externally occulted coronagraph, this is the external occulter. The diffraction off the IEO is both reflected and scattered reflected by the primary mirror (M1). The control of these two sources of stray-light is achieved in two ways. The diffraction off the IEO

- reflected by M1 is suppressed by stops (i.e., internal occulter and Lyot stop);
- scattered by M1 is controlled by minimizing the M1 surface roughness.

Stray light from the IEO not impinging on M1 can be either absorbed (the large majority) by the METIS structure or diffused: the latter, summed to all the other possible stray light contributions, has to be maintained to a level such to satisfy the provided stray light requirement.

METIS stray light requirement is very stringent and the stray light must be controlled at several stages of the instrument.
Table 2 summarizes the sources of stray light and how METIS is dealing with them and ***Fig. 4*** shows the comparison between the stray light estimate at 0.28 AU of S/C heliospheric distance with the expected coronal signal.

Table 2 - Stray light sources and METIS stray light rejection.

	Stray light source	**METIS Stray light rejection**
Direct solar disk light		
	Sun disk light entering IEO	Reflected back through IEO by M0
	Sun disk light scattered by M0	Reduced by black coating of the boom
	Sun disk light scattered by S/C components above IEO	Reduced by black coating on IEO
Sun disk radiation diffracted by IEO		
	Sun disk diffracted by IEO and reflected by M1	Blocked by IO
	IEO diffraction, diffracted by M0	Blocked by Lyot stop
	Sun disk diffracted by IEO and scattered by M1	Minimized with very highly polished M1

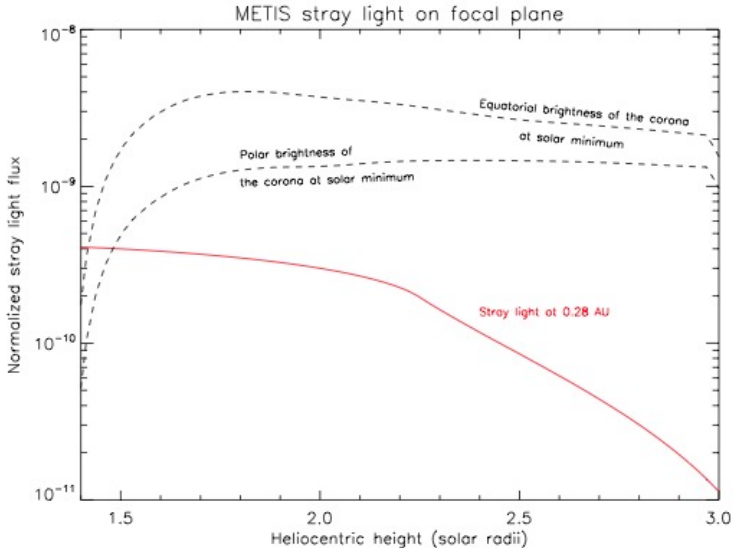

Fig. 4 - Comparison between stray light in VL and the expected coronal signal.

A. IEO design and characterization

The cone shape of the IEO has been chosen among other possible candidates for the external occulter, such as the simple aperture with a knife edge, multiple disks, serrated edge and truncated cones shapes, with different microroughnesses and colour.
The IEO shape, length, roughness and colour have been selected after a calibration campaign on several shapes of the IEO, carried on the boom occulter assembly (BOA) at both the Laboratoire d'Astrophysique de Marseille (LAM) and repeated at ALTEC/OPSYS in Turin to validate the future METIS test and calibration center [4].
represents an example of the shape of light diffracted by IEO onto the mirror M1 plane as a function of the mirror position with respect to the optical axis. A visual explaination of the shape of light is shown in ***Fig. 6*** where the tallest peak is given by the light diffracted by the external occulter, while, the second peak is given by the light that is reflected by the edge of the IEO. This second peak can be avoided if the telescope were longer than a meter-class coronagraph.

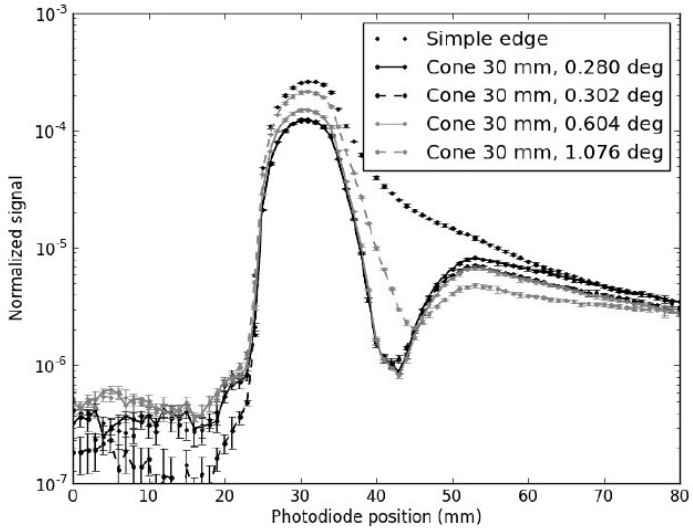

Fig. 5 - *Comparison between IEO shapes of IEO. Length 30 mm, black coating, 0.5 um roughness*

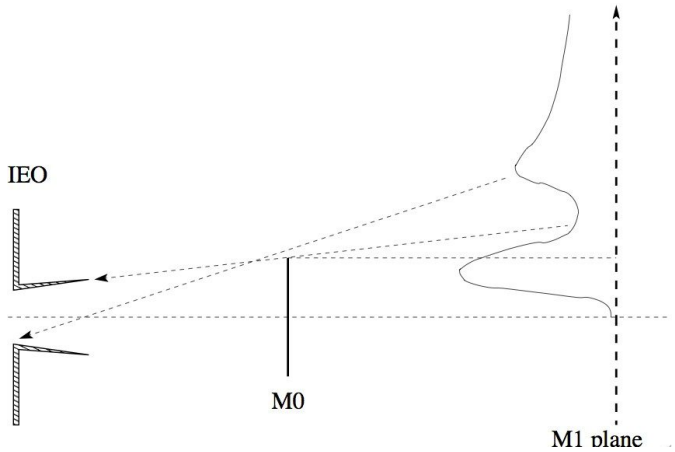

Fig. 6. - Sketch of the shape of the diffraction curve of IEO on the primary mirror.

B. Choice of coating

In order to define the best coating of the IEO internal surface, an investigation has been conducted on the performance of several black coatings. The measurement of the bidirectional reflectance distribution function (BRDF) was performed using a photogoniometer. The choice has fallen on the Acktar™ Black Magic.
BRDF measurements have been performed at LAM using the goniophotometer STIL S.A. mod.REFLET 180.
Hereafter, only the result of the BRDF measurement of Black Magic is shown. The full description of the characterization of several black coatings, among which Acktar™ Fractal, Carbon Fiber Reinforced Carbon (CFRC), Coblast™, Kepla-Coat®, and carbonitrides.

Table 3 - Computed Total Integrated Scatter (TIS) for each sample as a function of the incidence angle of the collimated beam

	TIS			
SAMPLES	$\theta_i = 5°$	$\theta_i = 30°$	$\theta_i = 50°$	$\theta_i = 70°$
Acktar Fractal™	4.0%	4.3%	5.3%	10.7%
Acktar Magic™	0.8%	0.9%	1.4%	5.2%
CFRC	6.6%	6.3%	6.9%	15.3%
COBLAST®	4.0%	4.1%	4.4%	4.9%
DLCg2	5.8%	5.5%	6.4%	14.2%
DLCg5	6.4%	6.1%	7.5%	18.6%
KEPLA-COAT™	6.0%	6.2%	7.3%	14.1%
TICNg5	8.67%	8.20%	9.44%	20.28%
PU1LAM	2.44%	2.56%	2.84%	3.50%

All these coatings have a scattering behavior close to lambertian with very low total integrated scatter (TIS). ***Table 3*** gives the TIS values measured by illuminating the sample with collimated beam at different incidence angles.
Data taken at discrete azimut angles have been interpolated in order to derive the full hemispheric BRDF using a cubic interpolation at constant angle of scattering. The result for Acktar™ Black Magic is shown in the elevation plot of ***Fig. 7***.

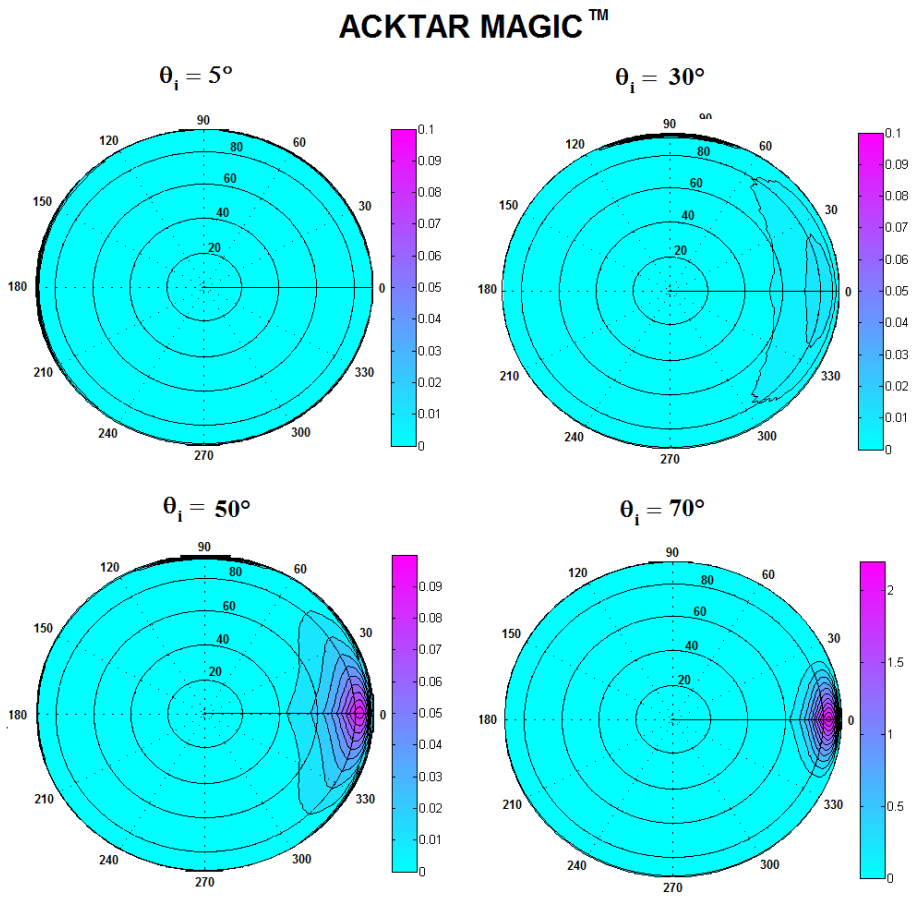

Fig. 7 – Acktar™ Black Magic BRDF hemispheric profile.

IV. METIS IN-FLIGHT OFF-POINTING

The Solar Orbiter mission profile foresees three 10 day length observing periods per orbit for the remote sensing instruments which are demanding in terms of resources, included telemetry. Each period is called Remote Sensing Windows (RSW) and includes the S/C pass through perihelion and maximum and minimum heliolatitude.

Outside the RSWs the RS instruments do not operate and METIS door will be closed.

During RSWs Solar Orbiter will be sun-center pointed with the exception of planned off-pointing windows to allow high resolution instruments to point targets on the disk upto the limb, and of S/C maneuvers such as wheel off-loading, high gain antenna maneuvers, breaks in fine guidance polynomials.

METIS, as a coronagraph, is designed to operate sun-centered. When the S/C is off-pointed METIS can operate with degraded performance upto a limit of off-pointing which is a function of the instrument parameters and of the heliocentric distance of Solar Orbiter.

Two limit angles, α_{max} and β_{max}, are defined, respectively, as the maximum angle of off-pointing at which, with degraded performance, it is possible to acquire scientific data, and as the maximum angle at which safety procedure are needed to protect the instrument.

As shown in ***Fig. 8***, α_{max} is the angle at which the solar disk radiation starts to illuminate the lateral surface of the IEO cone, while β_{max} is the angle at which M0 does not block the full disk light. ***Fig. 8*** provides also the numerical values of α_{max} and β_{max}, while ***Fig. 9*** shows the dependence of these angles from the S/C heliocentric distance.

Both angles take into account the absolute pointing error (APE) of both the S/C and METIS.

The ***Fig. 9*** displays also the size of the solar disk as a function of distance, showing that about 0.55 AU, the maximum allowed off-pointing exceeds the size of the Sun.

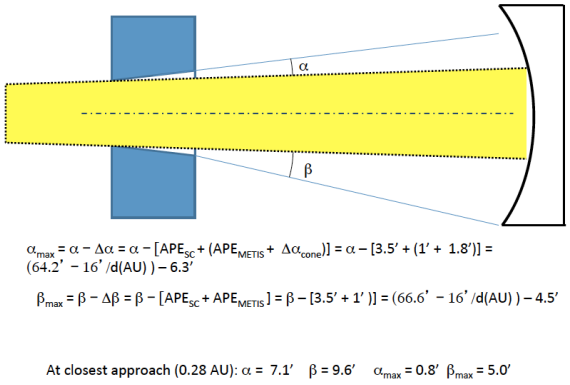

Fig. 8 - α_{max} and β_{max} definition.

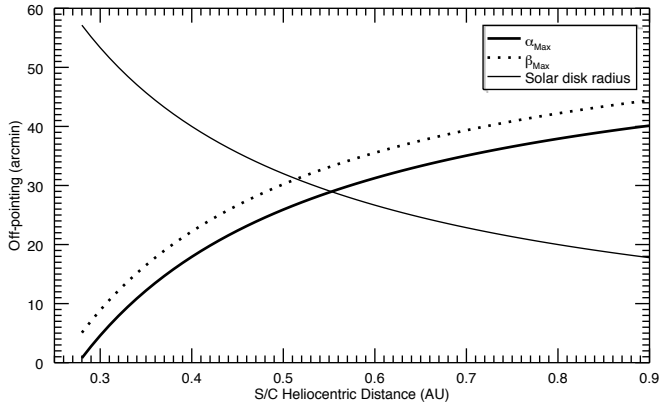

Fig. 9 - α_{max} and β_{max} as a function of the S/C heliocentric distance, with the size of the Sun disk.

Out of Sun center and within α_{max}, METIS can acquire science data with slightly degraded performance especially at lower heliocentric heights, close to the lower margin of the FOV, in the opposite direction of the offset pointing. The amount of degradation is given in ***Fig. 10*** where the ratio between the amount of diffracted light that reaches the primary mirror M1 from the edge of M0 with and without off-pointing is given as a function of the off-pointing. The data shown in ***Fig. 10*** are relative to the geometry of the boom occulter assembly breadboard (BOA) [4] representative of METIS boom geometry.

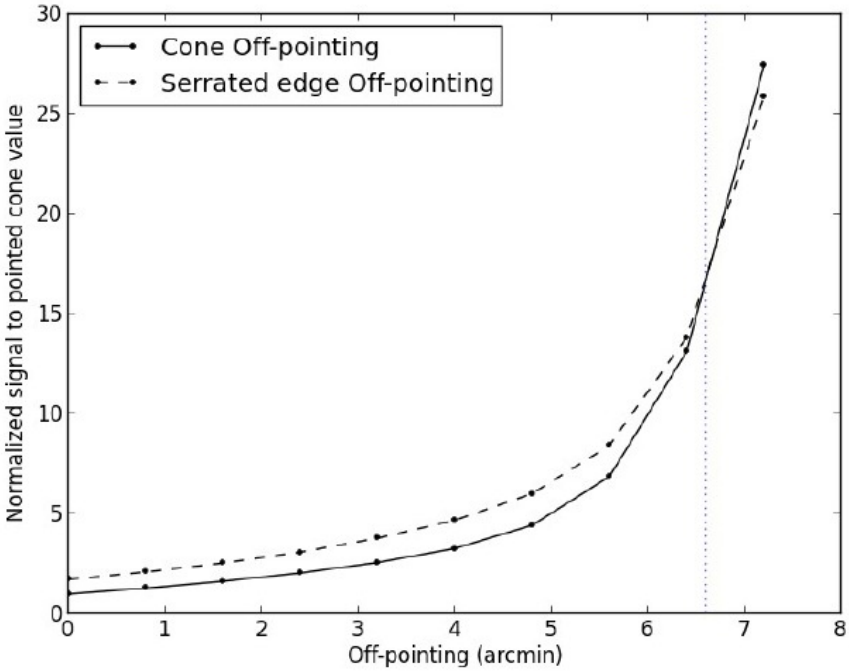

Fig. 10 - Total integrated diffraction comparison between a cone and a serrated edge as a function of coronagraph off-pointing. Data points are normalized to the total stray light in case the Sun center pointed cone. The vertical dotted line marks the limit where the Sun disk enters the telescope.

V. ACKNOWLEDGEMENTS

METIS Principal Investigator is Ester Antonucci. This work has been supported by the Italian Space Agency – ASI - under contract number I/013/12/0. The work of J.D. Moses has been supported by NASA NDPR NNH12AT2OI.

REFERENCES

[1] S. Fineschi et al., *Novel space coronagraphs: METIS, a flexible optical design for multi-wavelength imaging and spectroscopy*, Proceedings of the SPIE, Volume 8862, id. 88620G, 2013
[2] S. Fineschi, *Instrument Optical Performances Record,* Technical Report METIS-OATO-RPT-007, 29 May, 2014
[3] F. Landini et al, *Coating and surface finishing definition for the Solar Orbiter/METIS inverted occulter coronagraph,* Proceedings of the SPIE, Volume 9151, id. 91515H, 2014
[4] F. Landini, *METIS IEO Breadboard and Prototype Test Report*, Technical Report METIS-UNIFI-RPT-006, 7 March, 2014